Journal of Coordination Chemistry

ISSN: 0095-8972 (Print) 1029-0389 (Online) Journal homepage: http://www.tandfonline.com/loi/gcoo20

Spectroscopic studies on interactions of the tetrakis(acetato)chloridodiruthenium(II,III) complex and the Ru_2(II,III)-NSAID-derived metallodrugs of ibuprofen and ketoprofen with human serum albumin

Rodrigo Luis Silva Ribeiro Santos, Rute Nazaré Fernandes Sanches & Denise de Oliveira Silva

To cite this article: Rodrigo Luis Silva Ribeiro Santos, Rute Nazaré Fernandes Sanches & Denise de Oliveira Silva (2015) Spectroscopic studies on interactions of the tetrakis(acetato)chloridodiruthenium(II,III) complex and the Ru_2(II,III)-NSAID-derived metallodrugs of ibuprofen and ketoprofen with human serum albumin, Journal of Coordination Chemistry, 68:17-18, 3209-3228, DOI: 10.1080/00958972.2015.1074684

To link to this article: http://dx.doi.org/10.1080/00958972.2015.1074684

Accepted author version posted online: 21 Jul 2015.
Published online: 21 Aug 2015.

Journal of Coordination Chemistry, 2015
Vol. 68, Nos. 17–18, 3209–3228, http://dx.doi.org/10.1080/00958972.2015.1074684

Spectroscopic studies on interactions of the tetrakis(acetato) chloridodiruthenium(II,III) complex and the Ru_2(II,III)-NSAID-derived metallodrugs of ibuprofen and ketoprofen with human serum albumin

RODRIGO LUIS SILVA RIBEIRO SANTOS[1,2], RUTE NAZARÉ FERNANDES SANCHES[2] and DENISE DE OLIVEIRA SILVA*

Departamento de Química Fundamental, Instituto de Química, Universidade de São Paulo, São Paulo, Brasil

(*Received 6 April 2015; accepted 14 July 2015*)

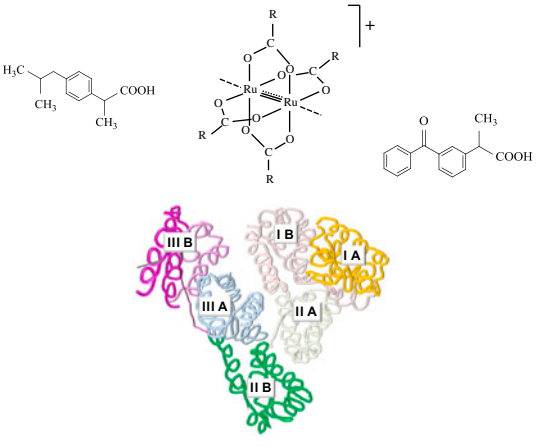

Diruthenium paddlewheel-structured complexes bearing a Ru_2(II,III) multiply bonded core show promising potential in medicinal chemistry. This work reports studies on the interactions of the tetrakis(acetato)chloridodiruthenium(II,III) complex (RuAc), $[Ru_2(\mu\text{-}O_2CCH_3)_4Cl]$, and the corresponding Ru_2(II,III)-non-steroidal anti-inflammatory drug (NSAID) metallodrugs of the NSAIDs ibuprofen (RuIbp) and ketoprofen (RuKet) with the human serum albumin (HSA). Circular dichroism (CD) studies showed that the three Ru_2 complexes interact with the HSA and induce conformational changes on the secondary structure of the protein. The reaction of the RuAc complex with the protein was monitored and the RuAc/HSA binding constant was estimated on the basis of electronic absorption spectroscopy data. Fluorescence emission spectroscopy studies were performed for all the Ru_2 complex/HSA systems and the Stern–Volmer constants and the thermodynamic parameters were

*Corresponding author. Email: deosilva@iq.usp.br
[1]Present address: Departamento de Ciências Exatas e Tecnológicas, Universidade Estadual de Santa Cruz, Rodovia Jorge Amado, Km 16, Ilhéus, BA, Brasil.
[2]These authors have contributed equally to this work.

determined for the RuAc/HSA binding. Mass spectrometry data confirmed the presence of the Ru_2 complexes in the protein phase after ultrafiltration. The studies suggest that the nature of the RuAc binding to the HSA is distinct from that of the derived RuIbp and RuKet metallodrugs. Electrostatic forces, accompanied by coordination of the metal to the amino acid side chains of the protein, seem to be the main forces acting in the RuAc/HSA binding, while non-covalent/hydrophobic forces might be predominant in the Ru_2-NSAID metallodrug/protein interactions. The findings suggest that the HSA protein might be a potential carrier in the blood plasma for the Ru_2(II,III)-NSAID metallodrugs.

Keywords: Diruthenium complexes; Anticancer metallodrugs; Ibuprofen; Ketoprofen; Human serum albumin

1. Introduction

Complexes bearing metal–metal multiple bonds have been theoretically and experimentally explored since their discovery by Cotton and coworkers [1]. The first evidence for a strong Ru–Ru bond in diruthenium tetracarboxylates appeared in 1969 [2], three years after the synthesis was reported by Stephenson and Wilkinson [3]. The known tetrakis(acetato)chloridodiruthenium(II,III) (or RuAc) of formula $[Ru_2(\mu\text{-}O_2CCH_3)_4Cl]$ displays a dimetallic center that contains two Ru ions directly connected in a short distance (2.28 Å) with a bond order of 2.5 [1, 4, 5]. The $[Ru_2(\mu\text{-}O_2CR)_4]^+$ unit [figure 1(a)] adopts the paddlewheel geometry stabilized by coordination of the Ru_2 core to four equatorial carboxylate bridging ligands. The chlorido-species, in which the chloride is axially coordinated to the Ru_2 core, display infinite polymeric chains linked by Ru–Cl axial bonds in the solid state [1]. Although the mixed-valence Ru_2(II,III) core exhibits formally oxidation states 2 and 3, it actually contains two equivalent metal ions in averaged oxidation state 2.5. The $[Ru_2]^{5+}$ core shows unusual stability that is assigned to the near-degeneracy of the two highest lying occupied molecular orbitals (π* and δ*), thus resulting in a $\sigma^2\pi^4\delta^2$ $(\delta^*\pi^*)^3$ ground state electronic configuration with a high spin state ($S = 3/2$) and three unpaired electrons per Ru_2 core [1, 6, 7]. The class of Ru_2(II,III) complexes shows unique structural, electronic,

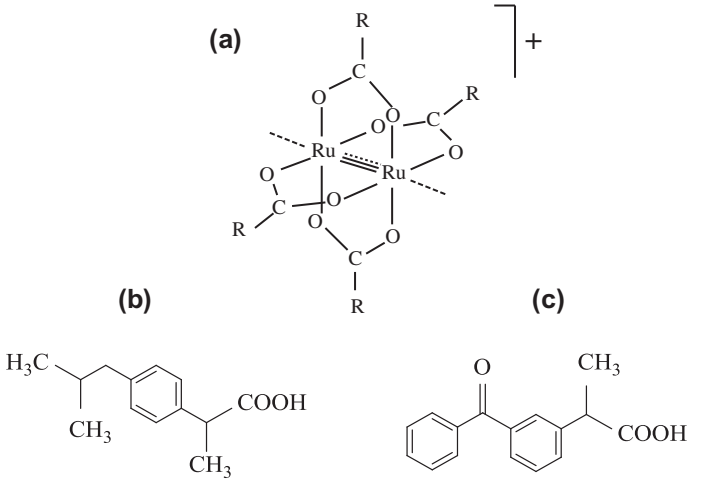

Figure 1. Structure of the $[Ru_2(\mu\text{-}O_2CR)_4]$+ paddlewheel unit (a), and structures of the non-steroidal anti-inflammatory drugs Ibuprofen, HIbp (b), and Ketoprofen, HKet (c), representing the racemic forms of the drugs.

spectroscopic, electrochemical, and magnetic properties, which account for potential applications in a variety of fields [1, 8, 9], including synthesis [1, 8, 10, 11], supramolecular/materials chemistry [12–19], biological chemistry [20–23], and catalysis [24–36].

In the context of the relevant role of ruthenium compounds in medicinal chemistry [see, e.g., 23, 37–43], we are interested in investigating the biological/pharmacological potential of the mixed-valence Ru_2(II,III) complexes. A novel class of melallodrugs containing the $[Ru_2(\mu\text{-}O_2CR)_4]^+$ unit, where the carboxylate anion derives from a pharmaceutical drug, has been prepared, characterized, and investigated for biological properties [22, 23, 44–50]. Notably, the diruthenium complex $[Ru_2(Ibp)_4Cl]$, or RuIbp, of the non-steroidal anti-inflammatory drug (NSAID) Ibuprofen (HIbp), figure 1(b), was found to show similar anti-inflammatory properties, but to cause reduced stomach ulceration, when compared to the HIbp parent drug. More interestingly, Ru_2–NSAID complexes are capable of inhibiting proliferation of glioma cancer cells. RuIbp was shown to exhibit anticancer activity *in vitro* (in rat and in human glioma cell lines) and also *in vivo*, thus revealing interesting properties for further studies targeting brain cancer therapy [47]. RuIbp and the analog complex of the Ketoprofen (HKet) ligand, figure 1(c), $[Ru_2(Ket)_4Cl]$ or RuKet, display mild anti-proliferative activity in Caco-2 and HT-29 colorectal cancer cells [50].

The biological role of ruthenium drugs is highly dependent on their interactions with a variety of biomolecule targets, which may (or not) be associated to pro-drug transformations (reduction–oxidation and/or ligand substitution reactions) in the physiological environment [23, 37]. Ru(III)-*N*-heterocyclic complexes currently in clinical trials, i.e., the NAMI-A anti-metastatic drug [51] and the KP1019 and NKP1339 [52] cytotoxic drugs, as well as Ru(II) organometallics [53, 54] have been suggested to undergo pro-drug transformations and protein binding. The reactivity of the Ru_2(II,III) paddlewheel framework with biomolecules has been exploited recently [55, 56]. The RuAc complex undergoes chloride/water axial ligand substitution reactions and the corresponding diaqua-species, $[Ru_2(\mu\text{-}O_2CCH_3)_4(H_2O)_2]^+$, are able to displace one water molecule by amino acid ligands, as shown for His, Cys, Trp, and Gly [55]. The diaqua-species also undergo chemical reactions with biological reductant agents, ascorbic acid or glutathione, which involve an axial water/bio-reductant substitution followed by a $[Ru_2]^{5+}/[Ru_2]^{4+}$ intramolecular electron transfer process that is accompanied by oxidation of the reductant [56]. The RuAc complex binds to the model protein hen egg-white lysozyme by exchanging two of the acetate ligands as shown by the crystal structure that displays two Ru_2 moieties bonded to Asp101 and Asp119 residues of the protein, respectively [57].

Blood plasma proteins are relevant biomolecule targets for metallodrugs in the blood stream. Human serum albumin (HSA), the most abundant serum protein (*ca.* 6×10^{-4} mol L^{-1} blood concentration), shows exceptional capacity for reversibly binding and transporting bioactive molecules from the blood stream to specific targets, thus acting as an important nanovehicle for low molecular weight molecules in the human body [58, 59]. HSA binding can strongly affect biodistribution, bioavailability, pharmacological efficacy, and toxicity of metallodrugs. The polypeptide contains 585 amino acids, there is a sole Trp residue (Trp214), and the Cys residues, except for Cys34-free thiol, form disulfide bridges. The HSA secondary structure is dominated by α-helices (68%) and the arrangement of three domains (I, II, and III), each one having two subdomains (A and B, composed by six and four α-helices, respectively), leads to a globular heart-shaped conformation. The binding sites are classified as I–V Sudlow's drug sites (according to the ligand affinity) [60] or as FA1–FA9 fatty acid sites (that binds a variety of drugs) [59] (figure 2). Hydrophobic pockets in subdomains IIA and IIIA are relevant binding sites for various compounds

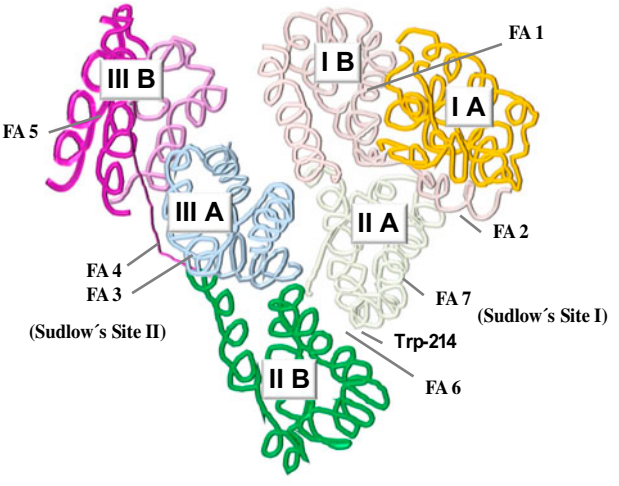

Figure 2. Schematic drawing representation of subdomains and binding sites of HSA. Domains I and II are almost perpendicular to each other. The interface region between IA and IB is connected to IIA by hydrophobic interactions and hydrogen bonds. Domain III interacts only with IIB, projecting out from it to give a Y-shaped assembly for II/III and shows few contacts with domain I due to the big channel created by IB/IIIA/IIIB. Sudlow's sites I and II are in subdomains IIA and IIIA, respectively. FA sites are FA1 (at IB), FA2 (at IA/IIA), FA3–FA4 (Sudlow's site II, at IIIA), FA5 (in a hydrophobic channel in IIIB), FA6 (IIA/IIB interface), FA7 (Sudlow's site I, at the hydrophobic cavity of IIA), FA8 (at the base of IA-IB-IIA/IIB-IIIA-IIIB gap), and FA9 (lying in an upper region of the same gap) (adapted from [58, 59, 78]).

[58, 59]. FA3–FA4 (Sudlow's site II, at subdomain IIIA) is the primary site for Ibuprofen, while FA6 and FA2 are the secondary and tertiary sites, respectively. FA7 (Sudlow's site I, at the hydrophobic cavity of IIA) binds the site marker warfarin. HSA can also bind a diversity of metal ions in at least three major metal-binding sites (N-terminal, free Cys34 thiol group, and cadmium site) [59]. Studies on interactions of albumin with the racemic forms and also with the enantiomeric forms of Ibuprofen [61–63] and Ketoprofen [64–66] by diverse techniques have been described.

The relevance of HSA as a biomolecule target, which plays a key role in the pharmacological properties and efficacy of ruthenium drugs, has been demonstrated [67]. Ru(III)-*N*-heterocyclic drugs in human trials, upon intravenous administration, can readily bind to the protein, following ligand exchange via its side chain (Hys and Cys) to form stable protein-bound adducts [52, 68]. Notably, differences in NAMI-A and KP1019 protein binding may account for their distinct biological activities and cellular uptake. NAMI-A binding to HSA has been suggested to involve covalent interactions. However, it has also been found that the Ru(II)-reduced form of the complex favors protein binding, although the reduction is disfavored for the covalently bonded in relation to the non-covalently bonded species (which are readily reduced by ascorbic acid) [68–71]. Conversely, the binding of KP1019 to HSA occurs mostly in a non-covalent manner, probably due to favorable interactions of the indazole ligands with the hydrophobic domains of the protein [72]. KP1019-HSA binding has been detected in blood samples from patients, showing that the albumin is the thermodynamically preferred binding partner in relation to transferrin [73–75]. KP1019 and its analog NKP1339 were found to bind sites I and II of HSA with moderately strong

affinity [76]. Moreover, HSA accumulates in tumor tissues and its recombinant form (rHSA) has been suggested as a carrier for ruthenium anticancer drugs [77].

Previous studies based on CD and SDS-PAGE performed in our laboratory suggested that the RuIbp metallodrug binds to HSA and induces conformational changes in the protein secondary structure without causing significant protein cleavage [46]. The present work extends our studies by investigating the interactions of the Ru_2(II,III) complexes, i.e., RuAc, RuIbp, and RuKet, with HSA. Electronic absorption spectroscopy is used to investigate the binding of the more soluble complex (RuAc) with the protein. Investigation of the interactions of the three Ru_2 complexes with the protein is conducted by CD and fluorescence emission spectroscopy. Mass spectrometry confirms the presence of the Ru_2 complexes in the protein phase after ultrafiltration experiments.

2. Materials and methods

2.1. *Materials*

All chemicals were of analytical reagent grade. Ruthenium(III) chloride, Ketoprofen (racemic), and other chemicals were purchased from Aldrich, except for Ibuprofen (racemic) that was from Natural Pharma manipulation pharmacy (São Paulo, Brazil). Solvents were from Merck or Synth suppliers. $[Ru_2(\mu\text{-}O_2CCH_3)_4Cl]$ [55], $[Ru_2(Ibp)_4Cl]$ [45], and $[Ru_2(Ket)_4Cl]$ [50] were prepared and characterized according to previously reported procedures. HSA was purchased from Sigma Aldrich and used without further purification. Stock solutions of HSA, freshly prepared in pH 7.4 physiological buffer (NaH_2PO_4 0.004, NaCl 0.100, $NaHCO_3$ 0.025 mol L^{-1}), were diluted with the buffer solution to the required concentrations and used immediately. The molar concentrations of the stock solutions of HSA were determined spectrophotometrically at 280 nm by using the molar absorptivity value of 3.6×10^4 mol^{-1} L cm^{-1} and the molecular weight of 66 kDa [79]. Deionized water was used throughout the experiments.

2.2. *Instrumentation*

The electronic absorption spectra were registered on a Shimadzu UV-1650 PC spectrophotometer equipped with thermostated cell holders from 190 to 1100 nm (electronic absorption spectroscopy studies for RuAc) or on a PerkinElmer Lambda 25 at 200–700 nm (inner filter correction). CD spectra were recorded on a JASCO J-720 (studies of interaction of HSA with the drugs, at 195–260 nm) or JASCO-815 spectropolarimeter (studies of the Ru_2 complexes, at 200–700 nm). Fluorescence spectra were recorded on a Varian Cary Eclipse spectrofluorimeter equipped with a Lauda Master Proline RP 845 thermostatic bath. Inductively coupled plasma–atomic emission spectroscopy (ICP–AES) analyses on a Spectro Ciros Arcos spectrometer, and matrix-assisted laser desorption/ionization time-of-flight mass spectrometry (MALDI-TOF-MS) analyses on a MALDI Ultraflextreme Bruker Daltonics equipment (with the matrices sinapinic acid and α-cyano-4-hydroxycinnamic acid (HCCA) for the *m*/*z* ranges of 20,000–200,000 and 800–4000, respectively) were performed at the Analytical Center of the Institute of Chemistry, University of São Paulo.

2.3. *Electronic absorption spectra studies*

In a first experiment, solutions of HSA (8.0×10^{-4} mol L^{-1}) and RuAc (8.0×10^{-4} mol L^{-1}) in pH 7.4 physiological buffer were mixed in a 1.0-cm tandem cuvette at 25 °C. The reaction was followed as a function of the time by recording the electronic absorption spectra from 200 to 1100 nm.

In a second experiment, solutions containing HSA (8.0×10^{-4} mol L^{-1}, pH 7.4) and variable concentrations (from 8.0 to 24.0×10^{-4} mol L^{-1}, pH 7.4) of the RuAc complex were incubated at 37 °C for 24 h. After that, the mixed solutions were transferred to a 1.0-cm cuvette and the electronic absorption spectra were recorded at 200–1100 nm. The value of the equilibrium constant (K) was determined by equation (1) [80]:

$$[P] + [L] = \varepsilon[P][L]/\Delta_{abs} - 1/K \quad (1)$$

where $[P]$ = HSA protein concentration, $[L]$ = Ru_2 complex ligand concentration, ε = molar extinction coefficient of the adduct, Δ_{abs} = absorbance changes at $\lambda = 545$ nm, and K = equilibrium constant for the reaction between P and L.

2.4. *CD measurements*

The protein solution (1.5×10^{-5} mol L^{-1}) was prepared by dissolving HSA in pH 7.4 physiological buffer. Solutions of RuAc dissolved in the physiological buffer and RuIbp, RuKet, HIbp, and HKet dissolved in ethanol were individually mixed with the HSA solution to give final concentrations of $1.5–7.5 \times 10^{-5}$ mol L^{-1} (Ru_2 complex) or $1.5–30.0 \times 10^{-5}$ mol L^{-1} (NSAIDs). The final concentration of ethanol was less than 2% v/v. After incubation at 37 °C during 24 h, the mixed solutions were transferred to a 1.0-mm quartz cuvette and the CD spectra were recorded at 195–260 nm. The mean residue ellipticity (MRE) or simply molar ellipticity (θ = ° cm^2 $dmol^{-1}$) values were calculated from equation (2) [81]:

$$\text{MRE}\,(\theta) = \text{CD}_{obs}/[P]\,nl\,10 \quad (2)$$

where MRE (θ) is mean residue ellipticity, CD_{obs} is the observed CD, $[P]$ is the protein molar concentration, n (= 585) is number of amino acid residues, and l is the path length. The estimated α-helix, β-content, and random contributions for the secondary structure of HSA were calculated using the K2d® software [82].

2.5. *Fluorescence measurements*

Fluorescence spectroscopic measurements were performed to follow changes on the protein emission band in the presence of the Ru_2 complexes. Appropriate volumes of stock solutions of RuAc in water (1.0×10^{-4} mol L^{-1}) and RuIbp and RuKet in ethanol (2.0×10^{-3} mol L^{-1}) were diluted with solution of HSA (2.0×10^{-6} mol L^{-1}, pH 7.4) to give final concentrations of $0–4.0 \times 10^{-5}$ mol L^{-1} (HSA : Ru_2 molar ratio from 1 : 0 to 1 : 20). The final concentration of ethanol was 2% (v/v). The mixed-component solutions were individually incubated at four distinct temperatures (10, 25, 37 and 45 °C) during 24 h. After that, the fluorescence emission spectra of the solutions in a 1.0-cm cuvette were recorded at 310–400 nm. The excitation wavelength was set at 295 nm to excite the Trp

214 residue selectively. A second experiment was performed in similar way, but at 37 °C for solutions of HSA (4.0×10^{-6} mol L^{-1}) containing RuIbp or RuKet concentrations that varied from 0.8 to 8.0×10^{-6} mol L^{-1} to give HSA : Ru_2 complex molar ratios at the range 1 : 0.2 to 1 : 2, respectively.

2.6. *Correction for inner filter effect*

The fluorescence intensities at the maximum emission wavelength were corrected for absorption of excitation light and reabsorption of emitted light (inner filter effect) with the basis on the absorption spectra data for each sample by applying equation (3):

$$F_{\text{corr}} = F_{\text{obs}} \times 10^{(A_{\text{em}}+A_{\text{exc}})/2} \tag{3}$$

where F_{corr} is the corrected emission intensity, F_{obs} is the recorded emission intensity, and A_{exc} and A_{em} is the solution absorbance at the excitation and emission wavelengths, respectively [83].

2.7. *Analysis of quenching mechanism*

The quenching experiments were carried out at four distinct temperatures (10, 25, 37, and 45 °C). The decrease in the fluorescence emission intensity was analyzed by the Stern–Volmer plot represented by equation (4) [83]:

$$F_0/F = 1 + k_q\tau_0[L] = 1 + K_{\text{SV}}[L] \tag{4}$$

where F_0 and F represent the fluorescence intensity in absence and presence of the quencher, respectively, k_q is the bimolecular quenching rate constant, τ_0 (10^{-8} s) is the lifetime of the unquenched fluorophore, $[L]$ is the concentration of the quencher ligand, and K_{SV} is the Stern–Volmer constant associated to the quencher–fluorophore interaction [84].

2.8. *Determination of the dissociation constant*

Dissociation constants were determined by the non-linear plot represented by equation (5) [85]:

$$F_0 - F = (F_0 - F_c) \times \frac{[P]_t + [L]_a + K_d - \sqrt{([P]_t + [L]_a + K_d)^2 - 4[P]_t[L]_a}}{2[P]_t} \tag{5}$$

where F_0 and F are the intensity emission of the protein in absence and presence of ligand, respectively, F_c is the fluorescence of the fully bound protein, $[P]_t$ is the total protein concentration, $[L]_a$ is the added ligand, and K_d is the dissociation constant. Equation (5), in contrast to the Stern–Volmer linear plot, is not limited to cases where the concentrations of free ligand and added ligand are approximately similar, and it can be applied for either decrease or increase of protein fluorescence when the ligand binds the fluorophore.

2.9. *Thermodynamic parameters determination*

The thermodynamic parameters ΔH, ΔG, and ΔS were calculated by equations (6) and (7) [66, 86]:

$$\ln K_{a2}/K_{a1} = 1/R(1/T_1 - 1/T_2)\Delta H \quad (6)$$

$$\Delta G = -RT \ln K_a = \Delta H - T\Delta S \quad (7)$$

where K_a is the binding constant at the corresponding temperature, ΔH, ΔS, and ΔG are the enthalpy, entropy, and free energy changes, respectively, and R is the gas constant. The temperatures (T) in Kelvin correspond to the experimental temperatures 10, 25, 37, and 45 °C.

2.10. *Ultrafiltration experiments*

Appropriate volumes of stock solutions of HSA (3.0×10^{-4} mol L^{-1}, pH 7.4 physiological buffer) and RuAc (3.0×10^{-3} mol L^{-1} in water) were mixed to give a final solution of 1.0×10^{-4} mol L^{-1} HSA and 1.0×10^{-3} mol L^{-1} RuAc (1 : 10 HSA : Ru_2 molar ratio). Appropriate volumes of stock solutions of HSA (6.0×10^{-5} mol L^{-1}, pH 7.4) and RuIbp or RuKet (1.0×10^{-3} mol L^{-1} in ethanol) were mixed to give a final solution of 2.0×10^{-5} mol L^{-1} HSA and 2.0×10^{-4} mol L^{-1} Ru_2–NSAID complex (1 : 10 HSA : Ru_2 molar ratio), having 20% (v/v) ethanol. All solutions were incubated at 37 °C for 24 h, and, after that, 3000 μL of each one was transferred to an Amicon® Ultra-4 30 K filter and centrifuged at 7000 rpm in a Hermle Z383 centrifuge for 2–4 min. The protein- or Ru bound-containing phase was washed twice with a solution of physiological buffer (pH 7.4, 20% ethanol). The experiment was performed in duplicate to separate samples for analysis. For ICP–AES analysis of Ru, the phase was quantitatively transferred to an Eppendorf tube, diluted to 2.0 mL with physiological buffer, and then diluted with hydrochloric acid 3.3%. The reliability and reproducibility of data obtained by this procedure were verified by performing parallel analysis for a second sample to which determined volumes (100 or 200 μL) of Ru atomic absorption standard solution (Aldrich) have been added before dilution. The % Ru was determined for both samples, and then, the % Ru of original sample was subtracted from % Ru of sample containing standard Ru, and the % recovered standard Ru was calculated. The values of % recovered standard Ru were found to be very close to the added standard Ru (higher than 90% recovery). For MALDI-TOF-MS spectrometry, the phase was diluted to 2.0 mL with physiological buffer.

3. Results and discussion

3.1. *Electronic absorption spectroscopic studies for RuAc*

3.1.1. Spectral changes of RuAc in the presence of HSA. The electronic absorption spectra of RuAc and HSA at 300–700 nm are shown in figure 3A(a) and (b), respectively. The band of RuAc at λ_{max} 424 nm is assigned to the π(Ru–O) → π^*(Ru_2) electronic transition. The shifting to higher energy in relation to the λ_{max} expected for the chlorido-species indicates predominance of the axially substituted $[Ru_2(\mu\text{-}O_2CCH_3)_4(H_2O)_2]^+$ diaqua-species

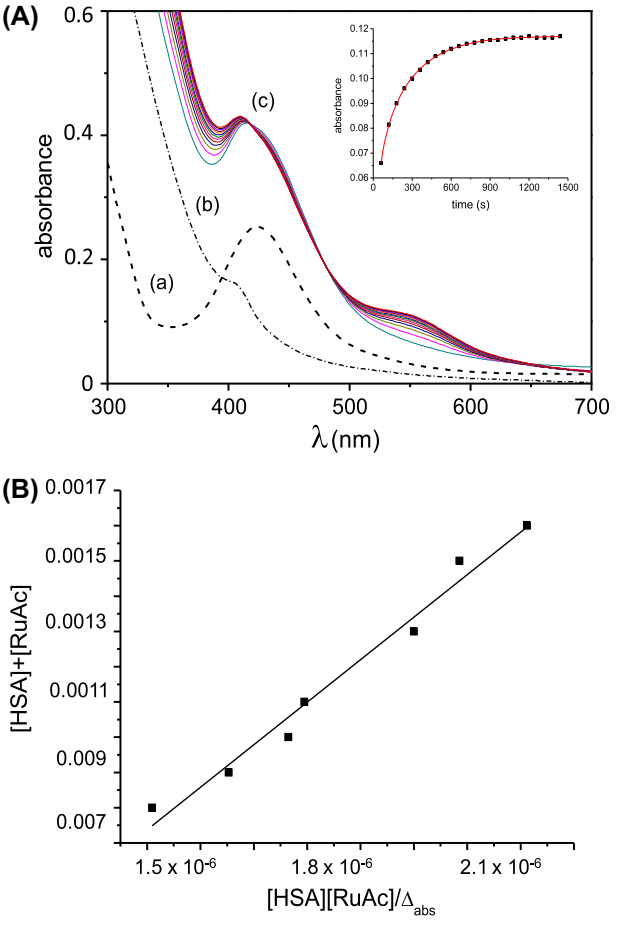

Figure 3. (A) Electronic absorption spectra of RuAc (4.0×10^{-4} mol L^{-1}) (a), HSA (4.0×10^{-4} mol L^{-1}) (b), and RuAc + HSA mixed solution (time scale 120–1500 s) (c), at 25 °C (pH 7.4). Insert: absorbance at 545 nm *vs*. time for reaction (c). (B) Linear plot of [HSA] + [RuAc] *vs*. $[HSA][RuAc]/\Delta_{abs}$ at $\lambda = 545$ nm for solutions of HSA (4.0×10^{-4} mol L^{-1}) and RuAc ($4.0–12.0 \times 10^{-4}$ mol L^{-1}) incubated at 37 °C for 24 h (pH 7.4).

in solution [55]. The spectrum of HSA at this region exhibits a shoulder at ~404 nm for which no assignment could be found in the literature. The two major bands of HSA are reported at ~220 nm, protein backbone transitions, and at 280 nm, arising from the phenyl rings in the amino acids Trp, Tyr, and Phe [87–90].

The spectral changes of a mixed solution of RuAc and HSA in equimolar concentrations were followed with time [figure 3A(c)]. The visible band of the Ru_2 complex shifted to higher energy ($\lambda_{max} \sim 416$ nm) while a new band appeared at 545 nm, accompanied by two isosbestic points (at 420 and 480 nm) which may suggest the presence of equilibrium species in solution. These spectral changes give evidence for interactions between RuAc and the protein. The shift of the visible band accompanied by lack of significant intensity decrease at 400–450 nm indicates that the $[Ru_2(\mu\text{-}O_2CCH_3)_4]^+$ paddlewheel framework is almost completely maintained in the presence of the protein. The appearance of a band at ~545 nm suggests that the RuAc diaqua-species interaction with albumin is likely to

involve, at least partially, axial ligand exchange with the protein amino acid residues. Similar spectral changes were observed in our previous studies showing that the $[Ru_2(\mu\text{-}O_2CCH_3)_4(H_2O)_2]^+$ species are capable of exchanging axially coordinated water with amino acids [55]. The binding of KP1019 to HSA was also reported to give a visible band, at ~580 nm [91, 92]. Moreover, the protein bindings of other ruthenium antitumor complexes involve amino acid residues, e.g., Ru(III) complex binding mostly involves His residues, while Ru(II)-arene complexes can bind to His, Met, and Cys residues on the surface of albumin [67, 93, 94].

The absorbance values at 545 nm were plotted as a function of time [figure 3(A), insert] showing no further significant changes after ~15 min reaction. Kinetic parameters could not be determined since it was not possible to follow the reaction under pseudo-first-order conditions due to the low solubility of the RuAc complex at the concentrations required for these studies. Nevertheless, the trace at 545 nm, at the present experiment conditions, led to estimate an observed rate constant of $\sim 10^{-3}\ s^{-1}$ magnitude order which is close to the magnitude of values reported for reactions of albumin with KP1019 ($3.3 \times 10^{-4}\ s^{-1}$) [95] and Ru(II) organometallics ($\sim 2 \times 10^{-4}\ s^{-1}$) [96].

3.1.2. Estimation of the equilibrium constant. A number of Benesi–Hildebrand-derived equations have been suggested for cases, such as low ligand/protein concentration ratio, in which the classical double-reciprocal plot fails in determining equilibrium constants [97–99]. Here, the equilibrium constant (K) was estimated by applying equation (1), since it is useful for cases where $[L] \sim [P]$, and RuAc and HSA were used in equimolar concentrations. In addition, a 1 : 1 binding system was assumed for the low concentration of the complex in this experiment. The absorbance values at 545 nm were measured for solutions of HSA containing variable concentrations of RuAc (1 : 1 to 1 : 3 HSA : RuAc molar ratio), which were previously incubated at 37 °C for 24 h. Spectral changes (not shown) indicated increase of the band intensity at 545 nm with increasing RuAc concentration. The values of [HSA] + [RuAc] were plotted against $[HSA][RuAc]/\Delta_{abs}$ [[figure 3(B)], and the equilibrium constant (K) for RuAc/HSA binding from the intercept of the linear plot was estimated as $9 \times 10^2\ mol^{-1}$ L. This value is lower than those ($\sim 10^4\ mol^{-1}$ L) reported for reactions of Ru(II)-organometallics with HSA [100, 101]. However, it approaches the equilibrium constant ($8.5 \times 10^2\ mol^{-1}$ L) found for the binding of albumin to the known cisplatin chemotherapeutic drug [102].

3.2. *CD studies*

CD was used to investigate secondary structural changes of HSA in the presence of the Ru_2 complexes or the NSAIDs. It is noteworthy to emphasize that the two Ru_2-NSAID complexes, RuIbp [55] and RuKet [56], already reported as metallodrugs by our group [22, 23], have been prepared from the corresponding HIbp and HKet racemic mixtures, i.e., equimolar mixtures of their two corresponding enantiomers, S(+) and R(−), which are the forms commercially available for drug administration. It may be supposed that the Ru_2-NSAID complexes have tendency to form non-chiral compounds in the solid state, since the crystal stereochemistry of the analog dimolybdenum-ibuprofen revealed that chiral ibuprofenate ligands (from HIbp racemic mixture) coordinate to the dimetallic core in a sequence that forms a $[Mo_2(R\text{-Ibp})_2(S\text{-Ibp})_2]$ centrosymmetric non-chiral complex [103]. The CD spectra of RuIbp and RuKet (in ethanol) were investigated and compared to the spectrum of the

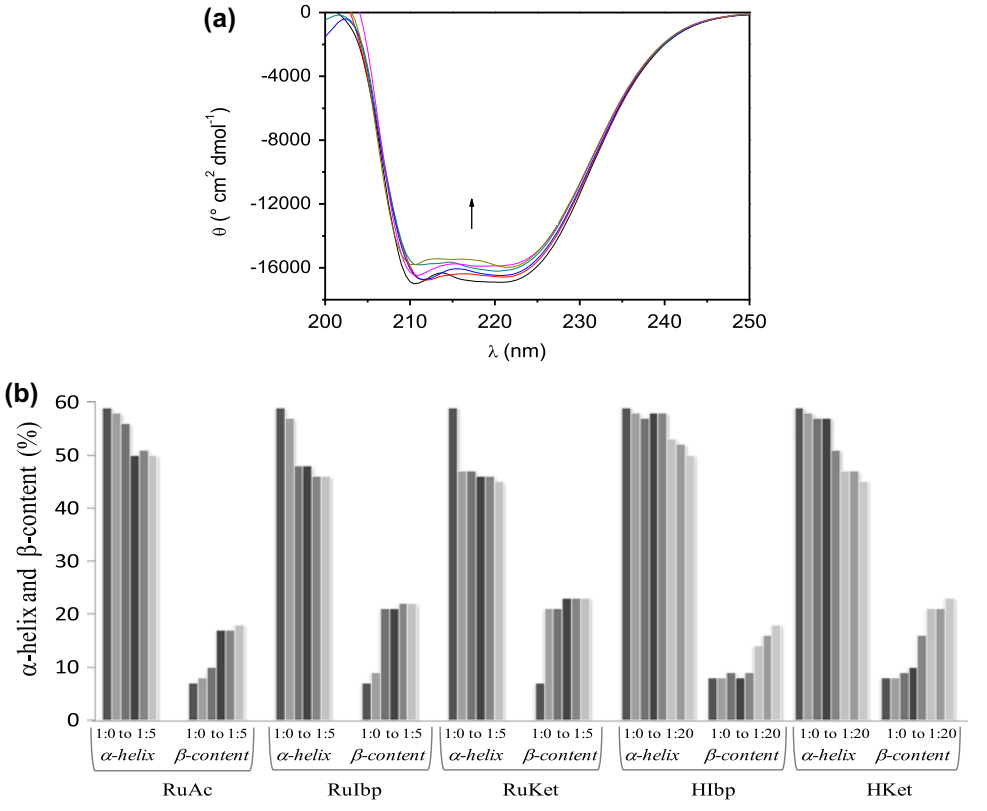

Figure 4. CD spectra showing the effects of increasing RuAc concentration (1.5–7.5 × 10^{-5} mol L^{-1}) in the HSA (1.5 × 10^{-5} mol L^{-1}) solution (corresponding to 1 : 0 to 1 : 5 HSA : RuAc molar ratios), after incubation at 37 °C for 24 h, pH 7.4 (a); α-helix and β-content contributions of HSA secondary structure in the presence of the Ru_2(II, III) complexes or the NSAIDs (HSA:NSAID molar ratio are in the sequence 1 : 0, 1 : 1, 1 : 2, 1 : 4, 1 : 8, 1 : 12, 1 : 16, 1 : 20).

non-chiral RuAc (in water). The CD spectra (not shown) of the three complexes were similar and showed no relevant signal at the UV and VIS regions that could indicate the presence of distinct stereoisomers in different relative concentrations for the RuIbp and RuKet complexes. Therefore, these findings give evidence that both Ru_2-NSAID metallodrugs show non-chiral behavior in solution.

The CD spectral changes of HSA in the presence of RuAc [figure 4(a)] and in the presence of the two Ru_2-NSAID complexes RuIbp, RuKet or the NSAIDs HIbp and HKet drugs (not shown) were very similar. The protein alone exhibits a typical CD spectrum with two negative UV bands (at 209 and 220 nm) which are assigned to the helical structure [104–106]. The addition of the Ru_2(II,III) complexes or the NSAIDs led to a decrease in intensity of the two protein bands, thus giving evidence for interactions that cause conformational changes in the HSA secondary structure. On the other hand, the resemblance in shape of all the CD spectra with that of HSA alone, along with the lack of any significant band shift, suggests that the protein secondary structure remains predominantly helical. The behavior shown by the Ru_2(II,III) complexes is distinct from that of other metal (ruthenium [92, 107], platinum [108], and rhodium [109]) complexes that cause HSA conformational changes with significant loss of helical stability.

The estimated α-helix and β-content contributions for the secondary structure of HSA in the systems investigated here are shown in figure 4(b). The random contribution (not shown) was almost constant with variation ≤3% in the range of 31–34% for all the cases. The contributions of α-helix and β-content for the secondary structure of HSA were found to be 59 and 7%, respectively, at the investigated experimental conditions. Upon addition of the Ru_2(II,III) complexes or the NSAIDs, a slight decrease in the α-helix contribution accompanied by an increase in the β-content was observed, while the random content was not significantly changed. Nevertheless, the α-helix loss was less than 15% for all the systems. The changes on the secondary structure of HSA were slightly dependent on the nature of the Ru_2(II,III) complex, achieving stabilization according to distinct HSA : Ru_2 complex molar ratios (1 : 3 for RuAc (50% α-helix, 17% β-content); 1 : 2 for RuIbp (48% α-helix, 21% β-content); and 1 : 1 for RuKet (47% α-helix, 21% β-content), with results for RuIbp that agree with our previous data [46]. The loss of α-helix content was slightly higher for the Ru_2(II,III)–NSAID complexes than for RuAc, thus giving evidence for the key role of the NSAID-derived ligand in interaction of the metallodrugs with the protein. On the other hand, the α-helix loss was higher for HIbp and HKet than for their corresponding metallodrugs when the NSAIDs were added to the protein solution at molar ratios corresponding to those of the NSAID-coordinated ligands in their respective complexes. The α-helix contributions were 58% at 1 : 8 HSA : HIbp molar ratio (that corresponds to 1 : 2 HSA : RuIbp) and 57% at 1 : 2 HSA : HKet molar ratio (that corresponds to 1 : 4 HSA : RuKet). Moreover, the α-helix content did not show decreased stabilization up to 1 : 20 HSA : NSAID molar ratio for both organic drugs. The distinct behavior of the Ru_2(II,III)-NSAID complexes in relation to their respective parent NSAIDs suggests that the protein interacts with the metallodrugs in a different manner than it interacts with the corresponding non-coordinated NSAIDs.

3.3. *Fluorescence spectroscopy studies*

3.3.1. Fluorescence quenching of HSA by RuAc. The changes of conformation of HSA in the presence of the RuAc complex were evaluated by measuring the intrinsic fluorescence of the sole tryptophan residue located in the hydrophobic pocket of subdomain IIA (Sudlow's site I). The fluorescence emission spectrum of HSA shows a strong band at $\lambda_{em} \sim 340$ nm (for excitation at λ_{exc} 295 nm) due to the Trp 214 chromophore. Changes of this emission give valuable information about the molecular environment surrounding the chromophore and have been used to follow HSA-drug binding affinity, thus providing evidence for interactions of drugs with the protein around the Trp pocket [105–107, 111,112].

The fluorescence emission spectrum of the protein was investigated in the presence of RuAc. The changes of intensity of the fluorescence band of HSA in the presence of RuAc are shown in figure 5(a). As the concentration of RuAc increased, the intensity of the protein emission decreased indicating a quenching process which suggests significant effects of the complex–protein binding on the conformation of the hydrophobic binding pocket in site I. Additionally, the lack of pronounced spectral shifts indicates that the protein folding is not significantly modified in the presence of the Ru_2(II,III) complex. This finding suggests a complex-protein binding that would be relevant from the viewpoint of transport properties of ruthenium drugs by the serum protein [113].

Analysis of possible fluorescence quenching mechanisms can be conducted on the basis of experiments at distinct temperatures, since the K_{SV} constants from the Stern–Volmer

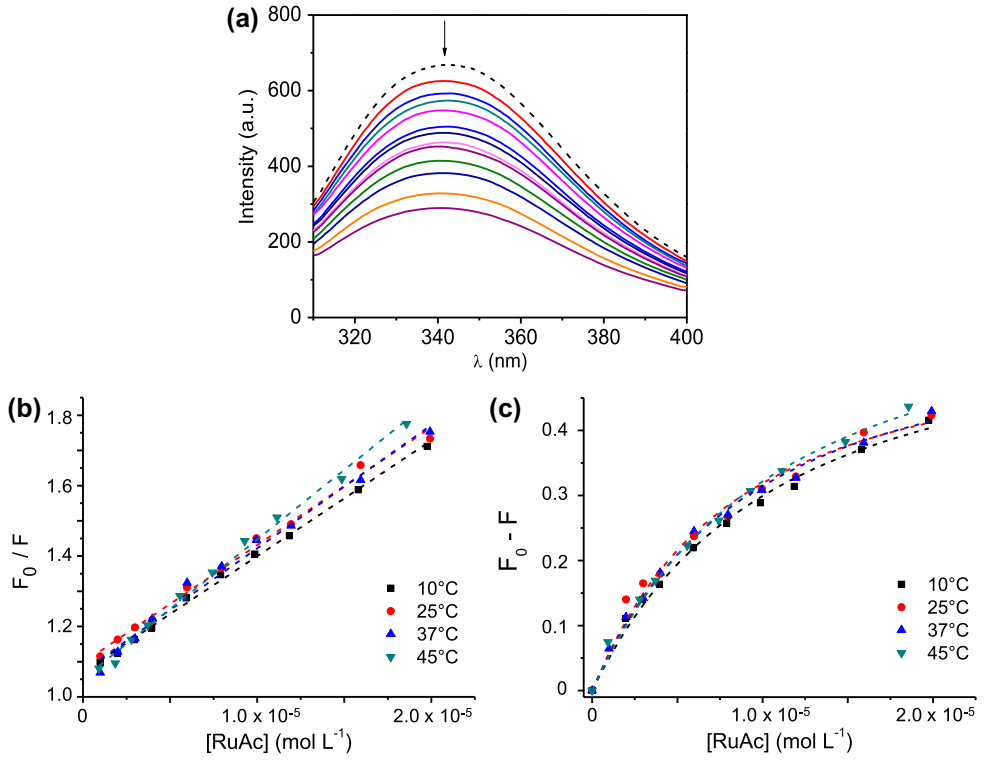

Figure 5. Fluorescence emission spectra of HSA (2.0×10^{-6} mol L^{-1}) (dashed line) and RuAc/HSA system, [RuAc] = 1.0, 2.0, 3.0, 4.0, 6.0, 8.0, 10.0, 12.0, 16.0, 20.0, 30.0, and 40.0×10^{-6} mol L^{-1} (solid lines), after incubation at 37 °C for 24 h, pH 7.4 (a). Stern–Volmer plots (b) and plots of ($F_0 - F$) *vs.* [RuAc] (c), for 1 : 0 to 1 : 10 HSA : Ru_2 molar ratios, at the temperatures 10, 25, 37, and 45 °C.

equation (4) show opposed dependence on temperature that distinguishes static and dynamic quenching mechanisms. In static quenching, a non-fluorescent quencher–fluorophore adduct is formed in the ground state, while in dynamic quenching, the quencher binds to the fluorophore during the lifetime of the excited state [84]. The stability of adducts usually decreases with increasing temperature, consequently decreasing the static quenching constant values. Higher temperatures favor larger diffusion coefficients, thus increasing the bimolecular quenching constant in the dynamic process [114]. In addition, the diffusional limit in collisional quenching leads to k_q maximum value of 2×10^{10} mol^{-1} L s^{-1} [110].

The values of F_0/F were plotted against [RuAc] according to equation (4) at the four temperatures (10, 25, 37, and 45 °C) [figure 5(b)] showing good linearity. The K_{SV} constants (table 1) for the RuAc/HSA binding system were determined by linear regression of the plots F_0/F *versus* [*L*], showing the same order of magnitude of those reported for other ruthenium drugs, e.g., KP1339 (4.6×10^4 mol^{-1} L, 25 °C) [70], NAMI-A (1.8×10^4 mol^{-1} L, 37 °C) [115], and different Ru(II) complexes (~10^4 mol^{-1} L) [101, 116–118]. The values of K_{SV} constant (table 1) increased slightly with increasing temperature in the presence of RuAc, suggesting a quenching process initiated by a dynamic mechanism. However, the calculated values of the k_q quenching rate constants (table 1) are of an order of magnitude (10^{12} mol^{-1} L s^{-1}) that is much higher than the maximum

Table 1. Stern–Volmer quenching constant (K_{SV}), quenching rate constant (k_q), dissociation constant (K_d), and thermodynamic parameters.

Complex	Calculated parameters	Temperature			
		10 °C/283 K	25 °C/298 K	37 °C/310 K	45 °C/318 K
RuAc	K_{SV} (10^4 mol^{-1} L)	3.29 ± 0.06	3.4 ± 0.1	3.5 ± 0.1	4.0 ± 0.1
	k_q (10^{12} mol^{-1} L s^{-1})	3.3	3.4	3.5	3.5
	R^2	0.9973	0.9925	0.9860	0.9938
	K_d (10^{-6} mol L^{-1})	9 ± 1	7 ± 1	7.8 ± 0.8	9 ± 1
	R^2	0.9944	0.9848	0.9953	0.9946
	ΔH (kJ mol^{-1})	−0.6	−12.6	−19.4	
	ΔS (J mol^{-1} K^{-1})	+94.3	+56.7	+35.3	
	ΔG (kJ mol^{-1})	−27.3	−29.5	−30.3	−30.6
RuIbp	nd	nd	nd	nd	nd
RuKet	K_{SV} (10^4 mol^{-1} L)	nd	nd	4.2 ± 0.2	nd
	k_q (10^{12} mol^{-1} L s^{-1})			4.2	
	R^2			0.9810	
	K_d (10^{-7} mol L^{-1})	nd	nd	3 ± 2	nd
	R^2			0.9870	

Notes: Data are expressed as mean of two measurements. nd = not determined value. R^2 = correlation coefficient adjusted R squared. F_c value was about 0.40 and 0.75 for RuAc and RuKet, respectively.

diffusion rate constant (10^{10} mol^{-1} L s^{-1}) of a fluorescence quenching initiated by adduct formation in a static process [83, 110, 119, 120]. The apparently contradictory behavior found for the RuAc/HSA system could be explained by considering an adduct which becomes more stable at high temperatures (at the investigated range) or that the mechanism is affected by the presence of fatty acids in the protein. The HSA used here contains fatty acids and globulins which may compete with the Ru_2(II,III) complex for the protein hydrophobic binding sites. In fact, there is evidence in the literature showing that the quenching mechanism may change from dynamic to static when ruthenium compounds bind to fatted HSA and HSA fatty acid free, respectively [121].

3.3.2. Determination of the dissociation constant for the RuAc/HSA system. The plots of ($F_0 - F$) *versus* [RuAc] [figure 5(c)] at distinct temperatures (10, 25, 37, and 45 °C) were used to determine the RuAc/HSA binding constant through the dissociation constant (K_d) from equation (5), by assuming the formation of 1 : 1 adduct at the low concentrations used here. The K_d constants (table 1) are 10^{-6} mol L^{-1} magnitude order, and closeness of values at all temperatures suggests that the stability of the RuAc/HSA system is mostly preserved at the investigated temperature range.

3.3.3. The nature of interaction forces for the RuAc/HSA binding system. The main forces in the binding process of a biomolecule binding to smaller species (ligand) may be different, comprising electrostatic, hydrogen bonds, van der Waals, or hydrophobic forces [122]. Protein association reactions with smaller species have been interpreted on the basis of a conceptual model consisting of two steps: The first one, related to mutual penetration of hydration layers with disordering of the solvent, consists of hydrophobic association and partial immobilization to form a hydrophobically associated protein–ligand, while the second following step involves short-range interactions to give the protein–ligand interacting

complex [123]. According to this model, the main forces in protein–ligand binding can be estimated from analysis of the thermodynamic parameters (ΔH, ΔS, and ΔG) associated to the binding process. Basically, for spontaneous process ($\Delta G < 0$), the acting forces in protein–ligand binding are predominantly electrostatic forces when $\Delta H < 0$ or $\Delta H \sim 0$ and $\Delta S > 0$, van der Waals forces or hydrogen bonds when $\Delta H < 0$ and $\Delta S < 0$, and hydrophobic interactions when $\Delta H > 0$ and $\Delta S < 0$ [123].

In the present work, the ΔH parameter was determined from equation (6), where the value of K_a was assumed to be $\sim 1/K_d$, and the reference temperature was 45 °C. The ΔG and ΔS parameters were determined by applying equation (7). The values of enthalpy change were relatively low and negative ($\Delta H < 0$) and the values of entropy change were positive ($\Delta S > 0$), while the free energy change was negative ($\Delta G < 0$), for all investigated temperatures at the present experimental conditions (table 1). These results indicate a spontaneous process that is driven by both enthalpy and entropy. According to the conceptual model for protein–ligand association [123], the low negative ΔH and the positive ΔS suggest electrostatic forces as the main binding forces in the RuAc/HSA system. In fact, this finding is in agreement with the predominant presence of the positively charged $[Ru_2(\mu\text{-}O_2CCH_3)_4(H_2O)_2]^+$ diaqua-species, which would be prone to interact with the protein in aqueous solutions of RuAc.

3.3.4. Effects of the Ru_2(II,III)-NSAIDs on HSA fluorescence changes. The changes on the conformation of HSA were investigated for the Ru_2-NSAID/HSA systems by monitoring the effects on the protein intrinsic fluorescence upon addition of the metallodrugs. Spectral changes (not shown) revealed a decrease in the fluorescence emission band of HSA with increasing Ru_2–NSAID concentration (at the range 1 : 0 to 1 : 20 HSA : Ru_2 molar ratio). This behavior might suggest fluorescence quenching of the protein emission by the complexes. The first analysis based on the fluorescence data without inner filter correction fitted equations (4) and (5) for the RuIbp/HSA system to give values of K_{SV} and K_d of order of magnitude $\sim 10^4$ mol^{-1} L and 10^{-6} mol L^{-1}, respectively. However, these data were found later to be not reliable since the HSA solutions containing RuIbp showed high absorption at the emission wavelength. In fact, the data after correction for absorption (inner filter) revealed an opposed effect, i.e., that the emission intensity actually increased with increasing Ru_2-NSAID concentration. Therefore, the high absorption (absorbance > 0.3 for HSA : Ru_2-NSAID molar ratio > 1 : 1.4) of the RuIbp–HSA solutions led to non-reliable data of binding constant from the Stern–Volmer plot at similar HSA : Ru_2 molar ratio range of that of the RuAc/HSA system. The RuKet/HSA system also showed high absorption at similar range of HSA : Ru_2 molar ratio.

In an attempt to minimize absorption problems, the experiments were performed for more diluted solutions of the complexes, at HSA : Ru_2-NSAID molar ratio range of 1 : 0.2 to 1 : 2. This study was conducted only at the temperature of 37 °C since it had the aim of estimating the binding constant rather than speculating quenching mechanisms. The data obtained for the RuIbp/HSA system at this molar ratio range also failed to determine binding constants. The changes on both F_0/F (equation (4)) and (F_0 − F) (equation (5)) values were insignificant, i.e., remaining almost constant, with increasing RuIbp concentration. These findings suggest that site I is unlikely to be the preferred site for the RuIbp binding to the protein. However, interactions in other sites may also cause conformational changes that disturb the Trp environment. The fluorescence emission data (not shown) at the same HSA : Ru_2-NSAID molar ratio range for the RuKet/HSA system fitted both equations (4)

and (5) to give K_{SV} and k_q values of ~10^4 mol^{-1} L and ~10^{12} mol^{-1} L s^{-1}, respectively, and calculated K_d value ~3×10^{-7} mol L^{-1}. Whereas the K_{SV} and k_q values were of similar magnitude to those found for the RuAc/HSA system, the K_d constant was approximately one order of magnitude lower at 37 °C (table 1). Therefore, it would be plausible to suggest that the Ru_2-NSAID/HSA systems are slightly more stable in relation to dissociation than the RuAc/HSA system system. Furthermore, these results might support the data obtained by CD studies which show that the Ru_2(II,III)–NSAID complexes exert more pronounced effects on the secondary structure of the protein, causing slightly higher loss of α-helix than RuAc, at similar HSA : Ru_2 molar ratios.

3.4. *Ultrafiltration and mass spectrometry experiments*

Mixed solutions of the Ru_2(II,III) complexes and HSA containing the Ru_2(II,III) complexes in 10-fold molar excess over the HSA, after incubation at 37 °C during 24 h, were submitted to ultrafiltration process to separate the non-bound Ru_2 species from the bound Ru_2 species interacting with the HSA. These experiments were performed in different conditions compared to the others since higher Ru_2 complex concentrations were used to investigate the maximum amount that could be retained in the protein phase. The high molecular weight protein phase after ultrafiltration was analyzed by ICP–AES and MALDI-TOF-MS spectrometry. The % Ru from ICP–AES indicated that approximately 70% of Ru_2 complex was retained in the protein phase in all three cases (RuAc, RuIbp, and RuKet). These results show high capacity of the protein phase in retaining the Ru_2(II,III) complexes at the investigated experimental conditions. Moreover, the nature of the equatorial ligand seems to not exert significant effects on the saturation capacity of the protein phase.

The MALDI-TOF-MS mass spectrum of the HSA alone (figure 6) shows two main peaks, at *m*/*z* 66,628 ($[HSA]^+$) and *m*/*z* 33,347 ($[HSA]^{2+}$), which are in agreement with the

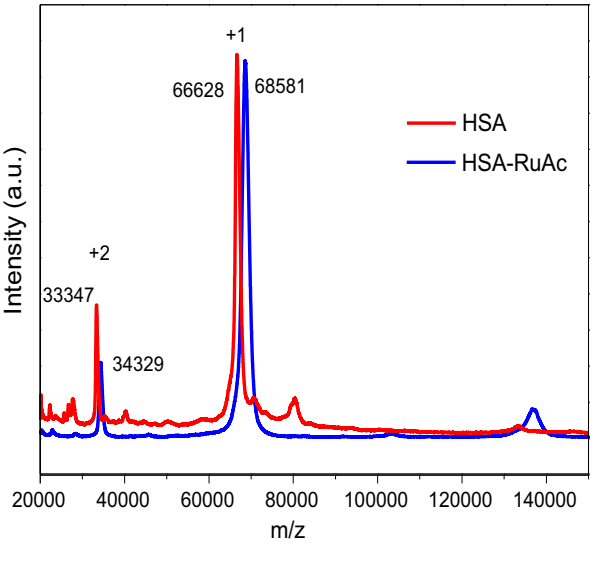

Figure 6. MALDI-TOF-MS spectra of HSA (1.5×10^{-4} mol L^{-1}) and RuAc/HSA system (1 : 10 HSA : RuAc molar ratio) in pH 7.4 physiological buffer, after incubation at 37 °C for 24 h, phase separated by ultrafiltration.

literature [124–129]. After incubation in the presence of RuAc, the two protein peaks shifted to higher *m/z* values (added *m/z*: 1953, $[M]^+$ and 982, $[M]^{2+}$) giving evidence for the presence of $[Ru_2(\mu\text{-}O_2CCH_3)_4]^+$ (439 Da) units. Conversely, the mass spectra of the Ru_2-NSAID/HSA systems (not shown) revealed small shifts of *m/z* values (~90 Da for RuIbp and ~550 Da for RuKet), in relation to the original peaks of the protein, which could not be assigned to any ruthenium species or even to free drug ligand. However, interesting data obtained from the MALDI-TOF-MS analysis at the lower *m/z* range. The RuIbp/HSA system showed a main peak at *m/z* 1024.26 with the isotopic pattern of ruthenium, which could be ascribed to the $[Ru_2(Ibp)_4]^+$ fragment (calculated *m/z* 1024.30), thus confirming the presence of the RuIbp complex in the high molecular weight protein phase after ultrafiltration. The RuKet/HSA phase, in contrast, did not present any peak that could be assigned to the $[Ru_2(Ket)_4]^+$ fragment. Nevertheless a set of peaks (at *m/z* 955.94, 1020.99, 1086.05, and 1151.10) could be associated to fragments of RuKet substituted-species, where the Ket ligands were exchanged with the α-cyano-4-hydroxycinnamate anion (HCC) of the matrix component α-cyano-4-hydroxycinnamic acid (HCCA) (i.e., $[Ru_2(HCC)_4]^+$, $[Ru_2(Ket)(HCC)]^+$, $[Ru_2(Ket)_4(HCC)_2]^+$, and $[Ru_2(Ket)_3(HCC)]^+$, at calculated *m/z* 955.95, 1021.00, 1086.05, and 1151.10, respectively). Similar fragments were also detected in the mass spectra (not shown) of the RuKet complex alone, thus confirming the presence of the original RuKet complex in the high molecular weight protein phase.

4. Conclusion

The three Ru_2(II,III) complexes, RuAc, RuIbp, and RuKet, bind HSA and induce conformational changes on the secondary structure of the protein. Fluorescence measurements indicate that the conformation of the hydrophobic binding pocket in subdomain IIA (site I) is affected by the presence of the compounds. The K_{SV} and k_q constants determined for the RuAc/HSA system suggest a quenching mechanism that might be initiated by dynamic process. Analysis of thermodynamic parameters points toward spontaneous process where electrostatic forces may play a key role in the RuAc/HSA binding, and the electronic spectral changes suggest metal coordination to the protein amino acid side chains. In contrast, the Ru_2(II,III)–NSAID complexes seem to interact with the HSA mostly through non-covalent/hydrophobic forces. These differences might be explained by considering that the voluminous NSAID anion ligands cause steric hindrance, thus making the axial sites in the $[Ru_2(\mu\text{-}O_2CR)_4]^+$ paddlewheel units of the metallodrugs less accessible to ligand substitution compared to RuAc. Moreover, the high hydrophobicity of the NSAID-derived ligands may favor interactions of the metallodrugs with the protein in its hydrophobic regions. The protein showed high capacity in retaining all the Ru_2(II,III) complexes after ultrafiltration. The findings suggest that HSA might be a potential carrier in the blood plasma for the Ru_2(II,III)–NSAID metallodrugs.

Acknowledgements

The authors gratefully acknowledge L.C.V. Rodrigues, H.F. Brito, E.L. Bastos, and R.R.P Santos for experimental and technical support.

Disclosure statement

No potential conflict of interest was reported by the authors.

Funding

This work was supported by Brazilian funding agencies Fundação de Amparo à Pesquisa do Estado de São Paulo (FAPESP) [grant numbers 2011/06592-1, 2014/23047-5], Conselho Nacional de Desenvolvimento Científico e Tecnológico (CNPq) [fellowship to Prof. D. de Oliveira Silva] and Coordenação de Aperfeiçoamento de Pessoal de Nível Superior (CAPES) [fellowships to R.L.S.R. Santos and R.N.F. Sanches].

References

[1] F.A. Cotton, C.A. Murillo, R.A. Walton. *Multiple Bonds Between Metal Atoms*, 3rd Edn, Springer Science and Business Media Inc., New York (2005).
[2] M.J. Bennett, K.G. Caulton, F.A. Cotton. *Inorg. Chem.*, **8**, 1 (1969).
[3] T.A. Stephenson, G. Wilkinson. *J. Inorg. Nucl. Chem.*, **28**, 2285 (1966).
[4] A. Bino, F.A. Cotton, T.R. Felthouse. *Inorg. Chem.*, **18**, 2599 (1979).
[5] T. Togano, M. Mukaida, T. Nomura. *Bull. Chem. Soc. Jpn.*, **53**, 2085 (1980).
[6] R.J.H. Clark, M.L. Franks. *J. Chem. Soc., Dalton Trans.*, **18**, 1825 (1976).
[7] J.G. Norman Jr, G.E. Renzoni, D.A. Case. *J. Am. Chem. Soc.*, **101**, 5256 (1979).
[8] M.A.S. Aquino. *Coord. Chem. Rev.*, **170**, 141 (1998).
[9] M.A.S. Aquino. *Coord. Chem. Rev.*, **248**, 1025 (2004).
[10] K. Dunlop, R. Wang, T.S. Cameron, M.A.S. Aquino. *J. Mol. Struct.*, **1058**, 122 (2014).
[11] E.G. Corkum, R. Wang, M.A.S. Aquino. *Inorg. Chim. Acta*, **424**, 202 (2015).
[12] T.E. Vos, Y. Liao, W.W. Shum, J.H. Her, P.W. Stephens, W.M. Reiff, J.S. Miller. *J. Am. Chem. Soc.*, **126**, 11630 (2004).
[13] W. Mori, T. Sato, C.N. Kato, T. Takei, T. Ohmura. *Chem. Rec.*, **5**, 336 (2005).
[14] G. Ribeiro, F.M. Vichi, D. de Oliveira Silva. *J. Mol. Struct.*, **890**, 209 (2008).
[15] M.C. Barral, R. González-Prieto, S. Herrero, R. Jiménez-Aparicio, J.L. Priego, E.C. Royer, M.R. Torres, F.A. Urbanos, F. Zamora. *J. Cluster Sci.*, **19**, 219 (2008).
[16] Z.D. Chaia, M.C. Rusjan, M.A. Castro, B. Donnio, B. Heinrich, D. Guillon, R.F. Baggio, F.D. Cukiernik. *J. Mater. Chem.*, **19**, 4981 (2009).
[17] B. Xi, T. Ren. *C. R. Chimie*, **12**, 321 (2009).
[18] M. Mikuriya, D. Yoshioka, A. Borta, D. Luneau, D. Matoga, J. Szklarzewicz, M. Handa. *New J. Chem.*, **35**, 1226 (2011).
[19] N.F. O'Rourke, M. Ronaldson, T.S. Cameron, R. Wang, M.A.S. Aquino. *J. Mol. Struct.*, **1052**, 17 (2013).
[20] B.K. Keppler. *Metal Complexes in Cancer Chemotherapy*, Wiley VCH, New York, NY (1993).
[21] C.E.J. van Rensburg, E. Kreft, J.C. Swarts, S.R. Dalrymple, D.M. Macdonald, M.W. Cooke, M.A.S. Aquino. *Anticancer Res.*, **22**, 889 (2002).
[22] D. de Oliveira Silva. *Anti Cancer Agents Med. Chem.*, **10**, 312 (2010).
[23] D. de Oliveira Silva. In *Frontiers in Anti-Cancer Drug Discovery*, Atta-ur-Rahman, M.I. Choudhary (Eds.), Vol. 4, Bentham Science Publishers, Sharjah (2014).
[24] P. Legzdins, R.W. Mitchell, G.L. Rempel, J.D. Ruddick, G. Wilkinson. *J. Chem. Soc. (A)*, 3322 (1970).
[25] A.J. Lindsay, G. McDermott, G. Wilkinson. *Polyhedron*, **7**, 1239 (1988).
[26] A.F. Noels, A. Demonceau, E. Carlier, A.J. Hubert, R.-L. Márquez-Silva, R.A. Sánchez-Delgado. *J. Chem. Soc., Chem. Commun.*, 783 (1988).
[27] N. Komiya, T. Nakae, H. Sato, T. Naota. *Chem. Commun.*, 4829 (2006).
[28] C.N. Kato, M. Ono, T. Hino, T. Ohmura, W. Mori. *Catal. Commun.*, **7**, 673 (2006).
[29] S.I. Murahashi, Y. Okano, H. Sato, T. Nakae, N. Komiya. *Synlett*, **2007**, 1675 (2007).
[30] C.N. Kato, W. Mori. *C. R. Chimie*, **10**, 284 (2007).
[31] J.E. Barker, T. Ren. *Inorg. Chem.*, **47**, 2264 (2008).
[32] Y. Kataoka, Y. Miyazaki, K. Sato, T. Saito, Y. Nakanishi, Y. Kiatagwa, T. Kawakami, M. Okumura, K. Yamaguchi, W. Mori. *Supramol. Chem.*, **23**, 287 (2011).
[33] L. Villalobos, J.E. Barkers Paredes, Z. Cao, T. Ren. *Inorg. Chem.*, **52**, 12545 (2013).
[34] T. Nakae, T. Yasunaga, M. Kamiya, Y. Fukumoto, N. Chatani. *Chem. Lett.*, **42**, 1565 (2013).
[35] S. Goberna-Ferrón, B. Peña, J. Soriano-López, J.J. Carbó, H. Zhao, J.M. Poblet, K.R. Dunbar, J.R. Galán-Mascarós. *J. Catal.*, **315**, 25 (2014).
[36] D.J. Thompson, J.E. Barkers Paredes, L. Villalobos, M. Ciclosi, R.J. Elsby, B. Liu, P.E. Fanwick, T. Ren. *Inorg. Chim. Acta*, **424**, 150 (2015).

[37] E. Alessio (Ed.). *Bioinorganic Medicinal Chemistry*, Wiley-VCH Verlag & Co KGaA, Weinheim (2011).
[38] G. Sava, A. Bergamo, P.J. Dyson. *Dalton Trans.*, **40**, 9069 (2011).
[39] A. Bergamo, C. Gaiddon, J.H.M. Schellens, J.H. Beijnen, G. Sava. *J. Inorg. Biochem.*, **106**, 90 (2012).
[40] C.G. Hartinger, N. Metzler-Nolte, P.J. Dyson. *Organometallics*, **31**, 5677 (2012).
[41] I. Romero-Canelón, P.J. Sadler. *Inorg. Chem.*, **52**, 12276 (2013).
[42] G. Süss-Fink. *J. Organomet. Chem.*, **751**, 2 (2014).
[43] A.A. Nazarov, C.G. Hartinger, P.J. Dyson. *J. Organomet. Chem.*, **751**, 251 (2014).
[44] A. Andrade, S.F. Namora, R.G. Woisky, G. Wiezel, R. Najjar, J.A.A. Sertié, D. de Oliveira Silva. *J. Inorg. Biochem.*, **81**, 23 (2000).
[45] G. Ribeiro, M. Benadiba, A. Colquhoun, D. de Oliveira Silva. *Polyhedron*, **27**, 1131 (2008).
[46] M. Benadiba, R.R.P. dos Santos, D. de Oliveira Silva, A. Colquhoun. *J. Inorg. Biochem.*, **104**, 928 (2010).
[47] M. Benadiba, I. de M. Costa, R.L.S.R. Santos, F.O. Serachi, D. de Oliveira Silva, A. Colquhoun. *J. Biol. Inorg. Chem.*, **19**, 1025 (2014).
[48] G. Ribeiro, M. Benadiba, D. de Oliveira Silva, A. Colquhoun. *Cell Biochem. Funct.*, **28**, 15 (2010).
[49] J.A. Miyake, M. Benadiba, G. Ribeiro, D. de Oliveira Silva, A. Colquhoun. *Anticancer Res.*, **34**, 1901 (2014).
[50] R.L.S.R. Santos, A. Bergamo, G. Sava, D. de Oliveira Silva. *Polyhedron*, **42**, 175 (2012).
[51] T. Gianferrara, I. Bratsos, E. Alessio. *Dalton Trans.*, 7588 (2009).
[52] C.G. Hartinger, S. Zorbas-Seifried, M.A. Jakupec, B. Kynast, H. Zorbas, B.K. Keppler. *J. Inorg. Biochem.*, **100**, 891 (2006).
[53] A.F.A. Peacock, A. Habtemariam, R. Fernández, V. Walland, F. Fabbiani, S. Parsons, R.E. Aird, D.I. Jodrell, P.J. Sadler. *J. Am. Chem. Soc.*, **128**, 1739 (2006).
[54] M.V. Babak, S.M. Meier, A.A. Legin, M.S.A. Razavi, A. Roller, M.A. Jakupec, B.K. Keppler, C.G. Hartinger. *Chem. Eur. J.*, **19**, 4308 (2013).
[55] R.L.S.R. Santos, R. van Eldik, D. de Oliveira Silva. *Inorg. Chem.*, **51**, 6615 (2012).
[56] R.L.S.R. Santos, R. van Eldik, D. de Oliveira Silva. *Dalton Trans.*, **42**, 16796 (2013).
[57] L. Messori, T. Marzo, R.N.F. Sanches, D. de Oliveira Silva. *Angew. Chem. Int. Ed.*, **53**, 6172 (2014).
[58] S. Sugio, A. Kashima, S. Mochizuki, M. Noda, K. Kobayashi. *Protein Eng.*, **12**, 439 (1999).
[59] G. Fanali, A. di Masi, V. Trezza, M. Marino, M. Fasano, P. Ascenzi. *Mol. Aspects Med.*, **33**, 209 (2012).
[60] G. Sudlow, D.J. Birkett, D.N. Wade. *Mol. Pharmacol.*, **11**, 824 (1975).
[61] D.S. Hage, T.A.G. Noctor, I.W. Wainer. *J. Chromatogr. A*, **693**, 23 (1995).
[62] J. Ghuman, P.A. Zunszain, I. Petitpas, A.A. Bhattacharya, M. Otagiri, S. Curry. *J. Mol. Biol.*, **353**, 38 (2005).
[63] X. Xiong, Q. Zhang, Y. Nan, X. Gu. *Luminescence*, **28**, 954 (2013).
[64] Z.D. Zhivkova, V.N. Russeva. *J. Chromatogr. B*, **714**, 277 (1998).
[65] F. Lagrange, F. Péhourcq, M. Matoga, B. Bannwarth. *J. Pharm. Biomed. Anal.*, **23**, 793 (2000).
[66] S. Bi, L. Yan, Y. Sun, H. Zhang. *Spectrochim. Acta, Part A*, **78**, 410 (2011).
[67] A.R. Timerbaev, C.G. Hartinger, S.S. Aleksenko, B.K. Keppler. *Chem. Rev.*, **106**, 2224 (2006).
[68] M.I. Webb, R.A. Chard, Y.M. Al-Jobory, M.R. Jones, E.W.Y. Wong, C.J. Walsby. *Inorg. Chem.*, **51**, 954 (2012).
[69] M. Brindell, I. Stawoska, J. Supel, A. Skoczowski, G. Stochel, R. van Eldik. *J. Biol. Inorg. Chem.*, **13**, 909 (2008).
[70] M.I. Webb, C.J. Walsby. *Dalton Trans.*, **40**, 1322 (2011).
[71] V. Novohradský, A. Bergamo, M. Cocchietto, J. Zajac, V. Brabec, G. Mestroni, G. Sava. *Dalton Trans.*, **44**, 1905 (2015).
[72] N. Cetinbas, M.I. Webb, J.A. Dubland, C.J. Walsby. *J. Biol. Inorg. Chem.*, **15**, 131 (2010).
[73] C.G. Hartinger, M.A. Jakupec, S. Zorbas-Seifried, M. Groessl, A. Egger, W. Berger, H. Zorbas, P.J. Dyson, B.K. Keppler. *Chem. Biodivers.*, **5**, 2140 (2008).
[74] C.G. Hartinger, B.K. Keppler. *Electrophoresis*, **28**, 3436 (2007).
[75] R. Trondl, P. Heffeter, C.R. Kowol, M.A. Jakupec, W. Berger, B.K. Keppler. *Chem. Sci.*, **5**, 2925 (2014).
[76] O. Dömötör, C.G. Hartinger, A.K. Bytzek, T. Kiss, B.K. Keppler, E.A. Enyedy. *J. Biol. Inorg. Chem.*, **18**, 9 (2013).
[77] W.H. Ang, E. Daldini, L. Juillerat-Jeanneret, P.J. Dyson. *Inorg. Chem.*, **46**, 9048 (2007).
[78] K.K. Park, J.W. Park, A.D. Hamilton. *Org. Biomol. Chem.*, **7**, 4225 (2009).
[79] S. Krimm, J. Bandekar. *Adv. Protein Chem.*, **38**, 181 (1986).
[80] B.K. Seal, H. Sil, D.C. Mukherjee. *Spectrochim. Acta, Part A*, **38**, 289 (1982).
[81] S.M. Kelly, T.J. Jess, N.C. Price. *Biochim. Biophys. Acta*, **1751**, 119 (2005).
[82] M.A. Andrade, P. Chacón, J.J. Merelo, F. Morán. *Prot. Eng.*, **6**, 383 (1993).
[83] J.R. Lakowicz. *Principles of Fluorescence Spectroscopy*, 3rd Edn, Spring Science and Business Media Inc., Baltimore, MD (2006).
[84] M.R. Eftink. In *Biophysical and Biochemical Aspects of Fluorescence Spectroscopy*, T.G. Dewey (Ed.), Plenum Press, New York (1991).
[85] M. van de Weert, L. Stella. *J. Mol. Struct.*, **998**, 144 (2011).

[86] I.M. Klotz, J.M. Urquhart. *J. Am. Chem. Soc.*, **71**, 847 (1949).
[87] Y. Liu, Q. Yu, C. Wang, D. Sun, Y. Huang, Y. Zhou, J. Liu. *Inorg. Chem. Commun.*, **24**, 104 (2012).
[88] Y. Wang, B. Tang, H. Zhang, Q. Zhou, G. Zhang. *J. Photochem. Photobiol. B*, **94**, 183 (2009).
[89] Z. Lu, Y. Zhang, H. Liu, J. Yuan, Z. Zheng, G. Zou. *J. Fluoresc.*, **17**, 580 (2007).
[90] W. He, Y. Li, C. Xue, Z. Hu, X. Chen, F. Sheng. *Bioorg. Med. Chem.*, **13**, 1837 (2005).
[91] F. Kratz, M. Hartmann, B. Keppler, L. Messori. *J. Biol. Chem.*, **269**, 2581 (1994).
[92] L. Trynda-Lemiesz, A. Karaczyn, B.K. Keppler, H. Kozlowski. *J. Inorg. Biochem.*, **78**, 341 (2000).
[93] A. Hnízda, J. Šantrůček, M. Šanda, M. Strohalm, M. Kodíček. *J. Biochem. Biophys. Methods*, **70**, 1091 (2008).
[94] W. Hu, Q. Luo, X. Ma, K. Wu, J. Liu, Y. Chen, S. Xiong, J. Wang, P.J. Sadler, F. Wang. *Chem. Eur. J.*, **15**, 6586 (2009).
[95] A.R. Timerbaev, A.V. Rudnev, O. Semenova, C.G. Hartinger, B.K. Keppler. *Anal. Biochem.*, **341**, 326 (2005).
[96] I. Berger, M. Hanif, A.A. Nazarov, C.G. Hartinger, R.O. John, M.L. Kuznetsov, M. Groessl, F. Schmitt, O. Zava, F. Biba, V.B. Arion, M. Galanski, M.A. Jakupec, L. Juillerat-Jeanneret, P.J. Dyson, B.K. Keppler. *Chem. Eur. J.*, **14**, 9046 (2008).
[97] K.A. Connors. *Binding Constants – The Measurement of Molecular Complex Stability*, John Wiley-Sons, New York (1997).
[98] P. Qureshi, R.K. Varshney, S.B. Sigh. *Spectrochim. Acta, Part A*, **50**, 1789 (1994).
[99] R.L. Scott. *Recl. Des Trav. Chim. Des Pays-Bas*, **75**, 787 (1956).
[100] F. Beckford. *Int. J. Inorg. Chem.*, **2010**, 1 (2010).
[101] F. Beckford, D. Dourth, M. Shaloski, J. Didion, J. Thessing, J. Woods, V. Crowell, N. Gerasimchuk, A. Gonzalez-Sarrías, N.P. Seeram. *J. Inorg. Biochem.*, **105**, 1019 (2011).
[102] J.F. Neault, H.A. Tajmir-Riahi. *Biochim. Biophys. Acta – Protein Struct. Mol. Enzymol*, **1384**, 153 (1998).
[103] F.A. Cotton, D. de Oliveira Silva. *Inorg. Chim. Acta*, **249**, 57 (1996).
[104] A. Rodger, B. Noiden. *Circular Dichroism and Linear Dichroism*, Oxford University Press, Oxford (1997).
[105] N.J. Greenfield. *Anal. Biochem.*, **235**, 1 (1996).
[106] H.N. Hou, Z.D. Qi, Y.W. OuYang, F.L. Liao, Y. Zhang, Y. Liu. *J. Pharm. Anal.*, **47**, 134 (2008).
[107] L. Trynda-Lemiesz, B.K. Keppler, H. KozłLowski. *J. Inorg. Biochem.*, **73**, 123 (1999).
[108] N. Ohta, D. Chen, S. Ito, T. Futo, T. Yotsuyanagi, K. Ikeda. *Int. J. Pharm.*, **118**, 85 (1995).
[109] L. Trynda-Lemiesz, F.P. Pruchnik. *J. Inorg. Biochem.*, **66**, 187 (1997).
[110] J. Jayabharathi, V. Thanikachalam, M. Venkatesh Perumal. *J. Lumin.*, **132**, 707 (2012).
[111] M.X. Xie, X.Y. Xu, Y.D. Wang. *Biochim. Biophys. Acta*, **1724**, 215 (2005).
[112] S. Bi, D. Song, Y. Tian, X. Zhou, Z. Liu, H. Zhang. *Spectrochim. Acta, Part A*, **61**, 629 (2005).
[113] C.P. Matos, A. Valente, F. Marques, P. Adão, M. Paula Robalo, R.F.M. Almeida, J.C. Pessoa, I. Santos, M.H. Garcia, A.I. Tomaz. *Inorg. Chim. Acta*, **394**, 616 (2013).
[114] Y.J. Hu, Y. Liu, R.M. Zhao, S.S. Qu. *Int. J. Biol. Macromol.*, **37**, 122 (2005).
[115] O. Mazuryk, K. Kurpiewska, K. Lewiński, G. Stochel, M. Brindell. *J. Inorg. Biochem.*, **116**, 11 (2012).
[116] Y. Liu, Q. Yu, C. Wang, D. Sun, Y. Huang, Y. Zhou, J. Liu. *Inorg. Chem. Commun.*, **24**, 104 (2012).
[117] A.I. Tomaz, T. Jakusch, T.S. Morais, F. Marques, R.F.M. de Almeida, F. Mendes, É.A. Enyedy, I. Santos, J.C. Pessoa, T. Kiss, M.H. Garcia. *J. Inorg. Biochem.*, **117**, 261 (2012).
[118] F. Beckford, J. Thessing, M. Shaloski, P.C. Mbarushimana, A. Brock, J. Didion, J. Woods, A. Gonzalez-Sarrías, N.P. Seeram. *J. Mol. Struct.*, **992**, 39 (2011).
[119] Y. Hu, Y. Liu, J. Wang, X. Xiao, S. Qu. *J Pharm. Biomed. Anal.*, **36**, 915 (2004).
[120] N. Bijari, Y. Shokoohinia, M.R. Ashrafi-Kooshk, S. Ranjbar, S. Parvaneh, M. Moieni-Arya, R. Khodarahmi. *J. Lumin.*, **143**, 328 (2013).
[121] T.S. Morais, F.C. Santos, T.F. Jorge, L. Côrte-Real, P.J.A. Madeira, F. Marques, M.P. Robalo, A. Matos, I. Santos, M.H. Garcia. *J. Inorg. Biochem.*, **130**, 1 (2014).
[122] D. Leckband. *Annu. Rev. Biophys. Biomol. Struct.*, **29**, 1 (2000).
[123] P.D. Ross, S. Subramanian. *Biochemistry*, **20**, 3096 (1981).
[124] Y. Ke, S.K. Kailasa, H.-F. Wu, Z.-Y. Chen. *Talanta*, **83**, 178 (2010).
[125] H. Wang, W. Huang, J. Orwenyo, A. Banerjee, G.R. Vasta, L.-X. Wang. *Bioorg. Med. Chem.*, **21**, 2037 (2013).
[126] J. Zhang, D. Chatterjee, P.J. Brennan, J.S. Spencer, A. Liav. *Bioorg. Med. Chem. Lett.*, **20**, 3250 (2010).
[127] S. Crobu, M. Marchetti, G. Sanna. *J. Inorg. Biochem.*, **100**, 1514 (2006).
[128] L. Frost, M. Chaudhry, T. Bell, M. Cohenford. *Anal. Biochem.*, **410**, 248 (2011).
[129] Y.J. Chiou, K.B. Tomer, P.C. Smith. *Chem. Biol. Interact.*, **121**, 141 (1999).